

DTIC 1990 0000

(2)

AD

TECHNICAL REPORT ARCCB-TR-90035

**EFFECTS OF NOTCH GEOMETRY AND MOISTURE
ON FRACTURE STRENGTH OF CARBON/EPOXY
AND CARBON/BISMALEIMIDE LAMINATES**

AD-A231 892

J. H. UNDERWOOD

I. A. BURCH

S. BANDYOPADHYAY

DECEMBER 1990

DTIC
ELECTED
FEB 25 1991
S B D



**US ARMY ARMAMENT RESEARCH,
DEVELOPMENT AND ENGINEERING CENTER
CLOSE COMBAT ARMAMENTS CENTER
BENET LABORATORIES
WATERVLIET, N.Y. 12189-4050**



APPROVED FOR PUBLIC RELEASE; DISTRIBUTION UNLIMITED

91 2 21 026

DISCLAIMER

The findings in this report are not to be construed as an official Department of the Army position unless so designated by other authorized documents.

The use of trade name(s) and/or manufacturer(s) does not constitute an official indorsement or approval.

DESTRUCTION NOTICE

For classified documents, follow the procedures in DoD 5200.22-M, Industrial Security Manual, Section II-19 or DoD 5200.1-R, Information Security Program Regulation, Chapter IX.

For unclassified, limited documents, destroy by any method that will prevent disclosure of contents or reconstruction of the document.

For unclassified, unlimited documents, destroy when the report is no longer needed. Do not return it to the originator.

SECURITY CLASSIFICATION OF THIS PAGE (When Data Entered)

DD FORM 1 JAN 73 1473 EDITION OF 1 NOV 68 IS OBSOLETE

UNCLASSIFIED

SECURITY CLASSIFICATION OF THIS PAGE (When Data Entered)

7. AUTHORS (Cont'd)

I.A. Burch and S. Bandyopadhyay
Materials Research Laboratories
Defence Science and Technology Organisation
Melbourne, 3032, Australia

20. ABSTRACT (Cont'd)

controlled moisture chamber; and a 4000-hour exposure in a natural tropical environment.

The tests were performed to investigate the following effects on fracture and mechanical properties and on micro and macrofailure mechanisms of the laminates:

1. Effects of notch width and length and ply orientation on trans-laminar fracture toughness were studied in 0/90 and 0/ \pm 60 carbon/epoxy laminates, including effects of notches produced by ballistic penetration.

2. Effects of extended exposure to moisture and sunlight on fracture and mechanical properties were studied in various 0/90 layups of carbon/bismaleimide laminates. A direct comparison of controlled chamber and natural tropical moisture effects was made for two materials.

3. The load-deflection macrobehavior of notched panels was noted and analyzed. Linear-elastic and J-integral analyses were used to determine critical values of stress intensity factor, K, at the onset of self-similar translaminar fracture. A simple splitting model was used to describe the interlaminar failure which competed with and often prevented the translaminar fracture.

4. Scanning electron microscope fractography was used to investigate and contrast the microfailure mechanisms of the laminates. The differences in micromechanisms between carbon/epoxy and carbon/bismaleimide were related to differences in the macrofracture behavior of the materials.

Analysis was performed of the test procedures used for determining fracture toughness and flexural strength and modulus. The methods used for fracture toughness and associated K, J, and displacement expressions were proposed for more general use in measuring translaminar fracture toughness of composites. Use of the four-point bending test for flexural strength and modulus revealed an error which can occur in this type of test that is not fully addressed in ASTM Method D-790.

UNCLASSIFIED

TABLE OF CONTENTS

	<u>Page</u>
ACKNOWLEDGMENTS	iii
OBJECTIVES	1
MATERIALS AND SPECIMENS	2
TEST METHODS	3
Environmental Exposure	3
Fracture Toughness Tests	4
Flexure Tests	6
DISCUSSION OF RESULTS	7
Fracture Toughness	7
Flexure Tests	12
SUMMARY	15
REFERENCES	17

TABLES

I. MATERIAL AND TEST CONDITIONS	19
II. SUMMARY OF FRACTURE TOUGHNESS TESTS	20
III. SUMMARY OF FLEXURAL STRENGTH AND FLEXURAL MODULUS TESTS	21
IV. PLY ORIENTATION EFFECT ON FRACTURE TOUGHNESS	22
V. ENVIRONMENTAL EFFECTS ON FRACTURE TOUGHNESS FOR CARBON/BISMALEIMIDE	23

ILLUSTRATIONS

1. Fracture toughness test arrangement	24
2. Flexural strength and modulus test arrangement	25
3. Load versus deflection behavior of notched tensile panels	26

	<u>Page</u>
4. Typical splitting of 0/90 and 0 ₂ /90 carbon/bismaleimide panels	27
5. Effects of notch configuration on fracture toughness for 0/90 carbon/epoxy	28
6. Photograph of 0/90 carbon/epoxy panel with ballistic penetration, pieced together after tensile loading to failure; penetrator also shown	29
7. Effects of notch radius on fracture toughness for 0/ \pm 60 carbon/epoxy; nominal 2a/W = 0.5	30
8. Low magnification SEM fractographs at notch tip: (a) 90/0 carbon/epoxy, little fiber pullout	31
(b) 90/0 carbon/bismaleimide, extensive fiber pullout	31
9. High magnification SEM fractographs 3 mm from notch tip: (a) 90/0 carbon/epoxy, predominantly failure of fiber bundles	32
(b) 90/0 carbon/bismaleimide, predominantly pullout of individual fibers	32
10. Load versus deflection behavior of flexure specimens	33
11. Rotation of loading pins relative to flexure specimens	34
12. Flexural stress versus specimen deflection showing correction for rotation	35

ACKNOWLEDGMENTS

This cooperative research of the Australian Defence Science and Technology Organisation (Materials Research Laboratories) and the U.S. Army Armament Research, Development, and Engineering Center (Benet Laboratories) was performed at Materials Research Laboratories under the auspice of The Technical Cooperation Plan.

The authors are pleased to acknowledge the work of W. Yaiser of Benet Laboratories in preparing the composite samples for the test; J. Hill of Materials Research Laboratories (MRL)-Innisfail, Australia in conducting the tropical exposure tests; D. Saunders of Aeronautical Research Laboratories (ARL), Melbourne, Australia in conducting the moisture-chamber tests, B. Baxter of MRL, Melbourne, in performing the ballistic penetration tests, and M. Butler of MRL in preparing the illustrations.



Accession For	
NTIS GRA&I	<input checked="" type="checkbox"/>
DTIC TAB	<input type="checkbox"/>
Unannounced	<input type="checkbox"/>
Justification	
By _____	
Distribution/	
Availability Codes	
Dist	Avail and/or Special
A-1	

OBJECTIVES

The primary objective of this work is to investigate the translaminar fracture behavior of carbon/epoxy and carbon/bismaleimide laminates, as affected by certain configurational and environmental conditions. Cross-ply laminates of the thickness and orientation shown in Table I were subjected to three types of environment and tested for fracture toughness, flexural strength, and flexural modulus. Flexural tests of this composite material type are commonly used to obtain design information for various applications. In contrast, fracture mechanics tests and analyses are not commonly used to describe translaminar fracture of composites; their use can be subject to criticism (ref 1). Because of this question of fracture mechanics use with composites, an additional objective of the work is to identify some material and test conditions for which fracture mechanics can be used to describe translaminar fracture behavior. This additional objective is closely related to the armament applications of the work here. Since preexisting damage must be assumed for many armament components, such as damage produced by ballistic penetration, translaminar fracture toughness is clearly a critical material property. This seems to be true for many military and aerospace applications.

While the investigation proceeded, some significant differences in fracture behavior became apparent, as described in upcoming sections. Therefore, a third objective was established to relate the differences in macroscopic fracture behavior based on load-displacement traces to the differences in microscopic fracture mechanisms observed from scanning electron micrographs of the fracture surfaces. If definitive relationships of this type could be made, they would help with decisions of practical importance, such as material selection and design of components, and also identify conditions for which fracture mechanics can be successfully used with composite materials.

It is emphasized that the objectives and related applications of this work deal with fracture of composite materials which is translaminal in basic nature, that is, with damage and continuing fracture proceeding across fibers and laminae, as shown in Figure 1. This is quite a different phenomenon from interlaminal fracture, in which crack growth occurs by delamination between laminae. A summary of some work on interlaminal fracture toughness testing was recently given by O'Brien and coworkers (ref 2).

MATERIALS AND SPECIMENS

As shown in Table I, two types of cross-ply laminates were tested: carbon/epoxy and carbon/bismaleimide. The carbon/epoxy was purchased from the 3M Company as a cured 0/90 sheet and a cured 0/ \pm 60 sheet, both of ply type SP-286/T2 using high strength fibers. Tensile panels, nominally 100 mm by 300 mm, were cut from the sheets for fracture toughness specimens as shown in Figure 1. The specimens for flexure tests were the broken halves from the fracture tests, using care to avoid damaged areas as shown in Figure 2. Fracture toughness and flexure tests of seven-layer laminates of carbon/epoxy were performed in three orientations; 0/ \pm 60, 0/90, and 90/0. The 0/90 and 90/0 specimens were cut at right angles from the same sheet.

The carbon/bismaleimide was Fiberite X-86 prepreg tape, cured at 180°C and 170 KPa pressure between 300 mm by 400 mm platens for 4 hours, followed by post-curing at 240°C for 6 hours. The 0-degree plies were G-40 high strength fibers; the 90-degree plies were G-50 high modulus fibers. Three fracture toughness specimens, nominally 90 mm by 300 mm, were made from each cured blank. The flexure test specimens were typically a 50-mm by 100-mm undamaged section of the fracture test specimen. Fracture toughness and flexure tests of eleven-layer

laminates of carbon/bismaleimide were performed in four orientations from two types of blanks: 0/90, 90/0, 0₂/90, and 90₂/0.

TEST METHODS

Environmental Exposure

The baseline exposure to environment before the tests was the so-called laboratory air exposure. This was simply typical laboratory conditions: 20°C and 50 percent relative humidity, for about three months in the case of carbon/bismaleimide and several years for the carbon/epoxy.

The moisture chamber exposure was accomplished at Aeronautical Research Laboratories (ARL), Melbourne, Australia. The specimens were exposed to 85°C and 97 percent relative humidity for 400 hours and then encapsulated in plastic. Careful weighing before exposure and just before testing showed the following increase in weight due to moisture adsorption:

0/90 specimens: 0.79 percent, 0.10 percent standard deviation

0₂/90 specimens: 0.67 percent, 0.15 percent standard deviation

Natural tropical environment exposure was accomplished at Materials Research Laboratories (MRL) - Innisfail, Queensland, Australia. The specimens were exposed in a horizontal orientation in an open setting a few miles inland from the ocean at a latitude of 17°S. The exposure was from 28 May through 10 November 1987 for a total of 4000 hours. Mean weather conditions for this period are typically 22°C and 79 percent relative humidity. Weighing before exposure and just before testing showed the following change in weight:

0/90 and 0₂/90 specimens: -0.02 percent, 0.03 standard deviation

Since the standard deviation is larger in magnitude than the indicated decrease in weight, a negligible decrease in weight is indicated. A fine loose powder

was observed on the top surface of the specimen following exposure. This powder is believed to be a product of degradation of the outer surface of bismaleimide and could explain the weight-change results.

Fracture Toughness Tests

The center-notch tensile panel shown in Figure 1 was chosen for fracture toughness tests of the thin sheet material because no compression stresses are present in this configuration, even for deep notches. Compression stresses must be avoided, both from the testing and application viewpoints. When testing thin carbon/polymer laminates, compression can lead to local fiber and overall structural buckling, either of which can ruin a test. In applications, compression is avoided for similar reasons. A test configuration similar to the center-notch tensile panel, which would be suitable due to lack of compression stress, is the double-edge-notch specimen, but this configuration does not relate as directly to a panel with an internal notch due to a ballistic penetration. Recent work (ref 3) described the use of a pressurized cylinder as a fracture toughness test configuration. This can meet the requirement of no compressive stress and is, of course, well-suited to pressure vessel applications.

Fracture toughness tests were performed for fifteen cases of material, notch configuration, and environment, as summarized in Figure 1 and Table II. Three or more replicates were performed for each case, using a displacement rate of 1 mm/minute. A comparison of results from two cases, 90/0 carbon/epoxy and 90/0 carbon/bismaleimide, was included in a recent summary of fracture mechanisms of composite laminates (ref 4). All of the results are described here in Table II and in subsequent figures and discussion. The notch used in most of the tests was cut with a jeweler's saw which produced a 0.3-mm wide kerf. The notch type was varied in the first four cases listed in Table II to determine

some effects of notch geometry. Notch radii, r , from 0.02 to 3.0 mm for 0/±60 carbon/epoxy were tested by using sharpened notches (with a razor blade) and blunted notches (by intersecting a drilled hole). Notch lengths with $2a/W$ from 0.3 to 0.7 for 0/90 carbon/epoxy were tested and the results were compared with those from a notch produced by an oblique penetration of a rifle projectile. A 5.5-mm diameter projectile with about 1000 m/s velocity was used at an angle of 77 degrees from normal incidence.

The expression used here for stress intensity factor, K , is based on the early Feddersen expression (ref 5) with a modification (ref 6) to account for eccentricity, e , of the crack center line relative to the specimen center line. The expression is as follows, with nomenclature defined in Figure 1:

$$K = [P/BW] [\pi a \sec(\pi a/(W-2e))]^{1/2} \\ 0 \leq a/W \leq 1 ; \quad e/W \leq 0.15 ; \quad h/W \geq 1.0 \quad (1)$$

The effects of crack eccentricity, e/W , and height-to-width ratio, h/W , on K are quite small (ref 6) and are well-represented by the above expression. All specimen dimensions were within the above ranges, and the calculation of K for the specimens is believed to be accurate within about one percent.

An expression for the crack surface displacement, u , shown in Figure 1 is available from Tada, Paris, and Irwin (ref 7) which fits the collocation results of Newman (ref 8) within 2.5 percent. A similar expression was developed here which fits the collocation results within 0.5 percent and is somewhat less complex, as follows:

$$uEB/P = -0.14(2a/W) - 1.04(2a/W)^2 + 0.21(2a/W)^3 - 2.14(\ln[1-2a/W]) \\ 0 \leq 2a/W \leq 1 ; \quad h/W \geq 1.0 \quad (2)$$

where E is elastic modulus and the other parameters are shown in Figure 1. This expression is believed to be accurate within about one percent.

Flexure Tests

Flexural strength and modulus tests were performed by four-point bend loading, as indicated in Figure 2. This test was chosen to avoid the more severe stress concentration effects of the single central load point in the three-point test. Note in Figure 2 that the support pins were free to rotate; the load pins were fixed to help maintain a repeatable test configuration. Flexural tests were performed for fifteen cases of material and environment, as summarized in Table III. Three or more replicates were tested for each case using a displacement rate of 6 mm/minute.

The expression used for flexural strength, S_B , follows directly from the usual definition of outer fiber stress in bending, using the nomenclature of Figure 2

$$S_B = 3 P X / W B^2 \quad (3)$$

where P is the total applied load. The expression for flexural modulus, E_B , is available from Roark and Young (ref 9)

$$E_B = P L^3 [3(X/L) - 4(X/L)^3] / [48 W B^3] \quad (4)$$

For the tests here, $X/L = 0.25$, and Eqs. (3) and (4) reduce to the expressions in ASTM Method D-790 for Flexural Properties of Unreinforced and Reinforced Plastics and Electrical Insulating Material. A potential problem was noted while analyzing the flexural modulus tests, which is not fully addressed in Method D-790. Some ratios of loading pin diameter-to-span can cause a significant nonlinearity in the load versus deflection curve. This can affect the results of flexure tests, as discussed in the upcoming section.

DISCUSSION OF RESULTS

Fracture Toughness

Material and Orientation Effects

The general fracture behavior of the two types of laminates is summarized in Table II and Figures 3 and 4. A greatly simplified description is that the carbon/epoxy gave linear load-deflection curves, low values of K_{max} , and only notch-plane deformation (Figures 3a and 3b), whereas the carbon/bismaleimide gave nonlinear load-deflection curves, higher values of K_{max} , and significant splitting out of the notch plane (Figures 3d and 3e, Figure 4). The exceptions to this description were the carbon/bismaleimide 90/0 (Figure 3c) and 90₂/0 specimens, which gave more linear curves, lower K_{max} values, and much less splitting than the other carbon/bismaleimide specimens.

The most prevalent orientation effect was the expected correspondence between fracture toughness and the number of 0-degree plies in the laminate. In Table IV, three observations of this effect can be made from the results. Note that the ratio of measured K_{max} from three sets of 0/90-type laminates is close to the ratio of 0-degree plies. The largest difference in these ratios was for 0/90 and 90/0 carbon/bismaleimide. This may be due to the fact that the 0/90 samples showed splitting and the 90/0 samples did not; this may have increased K_{max} for the 0/90 samples and affected the ratio of K_{max} for the comparison.

The splitting behavior, shown schematically in Figure 4, was associated with high values of K_{max} and also with extensive nonlinear strain energy dissipation by the specimen (see Figure 3e). The use of K_{max} as a measure of fracture toughness does not include the nonlinear effects, so calculations of applied J-integral were made for this purpose. The procedure followed that of

Rice, Paris, and Merkle (ref 10), who gave the following expression for applied J for a center-cracked panel, using the nomenclature of this report:

$$J = K^2/E + (A_p - P\delta_p/2)/B(W/2 - a) \quad (5)$$

where K is the applied stress intensity factor and A_p is the area under the curve following a given plastic displacement, δ_p (see Figure 3e). In this report, the nonlinear displacement is referred to as permanent displacement, since it is clearly different from the plastic deformation occurring in metals. The applied J at maximum load was calculated using Eq. (5), converted to K using $J = K^2/E$, and reported as shown in Table II. Note that, as expected from the load-displacement plots of Figure 3, the applied K values calculated from J at maximum load, designated K_{Jmax} , are significantly higher than the K_{max} values, which include only elastic strain energy. Applied J provides a measurement of fracture toughness for materials and orientations which display the important splitting behavior characterized by extensive permanent strain energy before failure.

The splitting behavior can be described in another manner. The approximately bilinear load versus displacement behavior of Figure 3e and the end result of the splitting as sketched in Figure 4 can be related. If, after considerable splitting, the load on the specimen were carried by only the material in the two unnotched ligaments, then a reduced apparent elastic modulus, E_A , would be produced which depended upon the notch length-to-specimen width ratio, $2a/W$, as follows

$$E_A/E = 1 - 2a/W \quad (6)$$

where E is the modulus of the unnotched and unsplit panel. The ratio of the reduced apparent modulus to the initial modulus in Figure 3e is 0.34, and the value of $(1-2a/W)$ for that specimen is 0.32. This relatively close agreement

supports the above model, which involves an unloading of the material above and below the notch and a bilinear load-displacement behavior. This bilinear elastic slope behavior may be a useful way to characterize splitting behavior during fracture testing of cross-ply laminates.

Notch Configuration Effects

Figures 5, 6, and 7 highlight some of the effects of notch length and notch root radius on the measured fracture toughness of carbon/epoxy panels. The effect of notch length over the range $0.25 \geq 2a/W \geq 0.70$ is shown in Figure 5 for 0/90 carbon/epoxy. Results are shown for two notch radii, $r = 0.30$ mm and 0.15 mm, produced using different saw blade sizes. Regression lines for each set of results show less change of K_{max} with $2a/W$ than there is scatter in the data. If there is any significance to the placement of the regression lines, the placement is as expected, that is, the K_{max} values are lower for lower root radius. Values of fracture toughness for 0/90 carbon/epoxy laminates are available from the literature which are in general agreement with the results in Figure 5. Mao (ref 11) reports center-notch fracture toughness of 20 to 26 MPa $\text{m}^{1/2}$ for $2a/W$ of 0.28 and 0.50, respectively.

Results from four panels with a bullet hole for a notch are compared in Figure 5 with the saw-cut notch results. Figure 6 shows one of the panels, pieced together after the test, and the projectile. Even though the root radius of the notch produced by ballistic penetration was considerably larger than the saw cuts, the K_{max} values were within the scatter of the saw-cut results. This indicates that for this material, damage from ballistic penetration can be essentially equivalent to that from relatively sharp notches.

The effect of notch root radius over the range $0.025 \geq r \geq 3.0$ mm on measured K_{max} is shown in Figure 7 for 0/ \pm 60 carbon/epoxy. The mean of the six

results for $r = 0.025$ and 0.3 mm is shown as the horizontal line. The K_{max} values for the $r = 3.0$ mm tests are significantly higher, which may indicate that higher toughness results from radii of this size. It may also be an indication of the relatively clean radius produced by a sharp 6.0-mm drill compared with the rough radius produced by a saw cut.

Environmental Effects

A comparison of fracture toughness results showing the effects of environment is given in Table V. Included in the table is a simple and direct test of statistical significance--comparing the difference in the mean value of K_{max} with the larger of the standard deviations for the two sets of results. For the 0/90 material, no significant difference in fracture toughness is indicated for either chamber or tropical exposure. Note, however, in Figure 3 that the permanent displacement for one of the 0/90 tropical exposure tests was considerably less than that for the 0/90 chamber test. This difference is reflected in the K_{Jmax} values in Table II, where the mean value for tropical exposure is 281 MPa $\text{m}^{1/2}$, lower than the values for laboratory and chamber exposure. The large standard deviation for this tropical exposure value is caused by the fact that the other two tropical results were much higher, in the same range as the laboratory and chamber results.

The only significant difference in results clearly attributed to environment is the lower K_{max} for 0₂/90 material due to moisture chamber exposure, as shown in Table V. The difference in mean K_{max} is about thrice the amount of the larger standard deviation. In addition, referring to Table II, K_{Jmax} is significantly lower for the 0₂/90 chamber results than for the laboratory results. This indicates that the amount of permanent displacement sustained before failure is reduced as a result of moisture chamber exposure. Note in Table II

that the same was true following tropical exposure, but the $K_{J\max}$ values which showed this decrease following tropical exposure included considerable scatter.

Failure Mechanisms

The drastic differences in macrofracture behavior of the two types of laminate, as summarized in Table II and Figure 3, led us to look for concomitant differences in the micromechanisms of fracture. Bandyopadhyay and Murthy (ref 12) described experiments and models of failure mechanisms in glass/polyester materials. The approach here was to study the fracture surfaces using scanning electron microscopy. Figures 8 and 9 show some key results. The low magnification fractographs of Figure 8 show the fracture surface ahead of the notch and the notch tip at the left for 90/0 laminates of each type. The fracture surfaces are as drastically different as the fracture toughness results. The carbon/epoxy is relatively flat and featureless with no evidence of individual fiber pullout, whereas the carbon/bismaleimide is a severely contorted surface due primarily to extensive fiber pullout.

Higher magnification fractographs in Figure 9 show that the only evidence of pullout for the carbon/epoxy is a limited amount of pullout of fiber bundles before failure of the intact bundles. In contrast, extensive individual fiber pullout is observed for carbon/bismaleimide. Individual fiber pullout involves significantly more interfacial area and therefore is expected to result in more dissipation of energy during fracture and a higher fracture toughness. It is interesting to note that Evans and Marshall (ref 13) presented fractographs nearly identical in appearance to Figure 9b but from a ceramic/ceramic composite which showed greatly improved toughness over that of the ceramic matrix. They attributed the increase in toughness to the same mechanism under discussion here--extensive individual fiber pullout and related dissipation of energy.

Flexure Tests

General Behavior

Typical load versus deflection plots obtained from the two types of laminate are shown in Figure 10. A clear difference in the two materials was seen in the final failure behavior. The carbon/epoxy specimen shown failed abruptly (typical of all tests) at the point of contact of one or both of the load pins. The carbon/bismaleimide specimens often showed load variations corresponding to progressive failure through the thickness. This distinction between abrupt and progressive failure was generally the same as that observed in fracture testing, as shown in Figure 3.

Correction for Rotation

The plots of all flexure tests had one disturbing feature in common, that is, a continuously increasing slope. This was not the usual toe region nonlinearity, as described in ASTM Method D-790, because it continued until failure. The cause of the nonlinearity was found to be the rotation of specimen relative to the loading and support pins, as sketched in Figure 11. Using plane geometry it can be shown that the initial moment span, X , is changed due to rotation of pins relative to specimen to a smaller value, X_r

$$X_r = X - D \sin \alpha \quad (7)$$

where D is the pin diameter and α is the angle of rotation. For small angles, $\alpha = \delta/X$ and an expression for X_r/X is

$$X_r/X = 1 - \delta D/X^2 \quad (8)$$

where δ is the specimen deflection, as shown in Figure 2. For the carbon/epoxy test in Figure 10a for example, with $\delta = 3.3$ mm, $D = 12.5$ mm, and $X = 12.5$ mm, the ratio of actual-to-calculated moment span, X_r/X , is 0.74. This 26 percent decrease in the moment span would be directly reflected in flexural strength,

S_B , determined from the test, if Eq. (3) were used with no modification for rotation. In the results here, Eqs. (8) and (3) were combined to include rotation effects in the calculation of S_B . The flexural modulus was calculated from the slope at a load of 0.3 KN, at which point there is little effect of rotation on the slope, so no modification was used.

A review of ASTM Method D-790 showed that although the above-mentioned rotation error is reduced by the requirement of a maximum pin size, some significant errors are still possible. For example, for the test of Figure 10a using the $D = 6.0\text{-mm}$ maximum pin size specified in Method D-790, the value of X_p/X is 0.87, indicating that a 13 percent error in calculation of flexural strength would still occur.

A further demonstration of the need to correct rotation errors in flexural tests is given in Figure 12. The rotation correction given in Eq. (8) was applied to the results of Figure 10a, and plots of uncorrected and corrected flexural stress are compared. Note that the corrected values are very nearly a straight line, as expected for a linear elastic test, and that the corrected flexural strength is much reduced.

Corrected Results

The corrected flexural strength results and the flexural modulus results are listed in Table III. A general comparison with these results can be made from published data for various quasi-isotropic carbon/epoxy laminates; with no environmental effects, flexural strengths of about 500 MPa and moduli of about 50 GPa are typical (ref 14) and in reasonable agreement with results reported here. Ply orientation effects on strength and modulus are as expected in the results of Table III, that is, strength and modulus are closely related to the number of 0-degree plies.

One result of flexural modulus can be compared with a modulus value determined from a tensile panel. One of the carbon/epoxy specimens whose mean flexural modulus was 85.0 GPa (see Table III) was also instrumented so that the modulus could be measured as part of the fracture toughness test. Small aluminum blocks were bonded to the specimen surface about 5 mm above and below the notch center line to accommodate a clip gage of the type used in ASTM Standard Test Method for Plane-Strain Fracture Toughness of Metallic Materials, E-399. The slope of the plot of this displacement, u , (see Figure 1) versus load was used with Eq. (2) and the specimen dimensions to calculate a modulus of 34.3 GPa. The significantly higher value in bending (85.0 GPa) is a reflection of the dominance of the outer layers of a laminate in determining flexural modulus. This is particularly true for the relatively thin, seven-ply laminate under discussion in which the outer layers make up a larger share of the thickness than in a thicker laminate.

The effect of environment on flexural properties of carbon/bismaleimide was investigated for three ply orientations, 0/90, 0₂/90, and 90₂/0 (see Table III). No significant effect on flexural modulus was found; some lower values were noted following environmental exposure, but the differences were smaller than the standard deviations. A statistically significant decrease in flexural strength was found for the 0₂/90 material following moisture chamber exposure (0.67 percent weight increase due to 85°C and 97 percent relative humidity exposure). The mean strength decreased from 486 to 397 MPa, an 18 percent drop. These results can be compared to typical data from the literature (ref 14) for carbon/epoxy, which can absorb up to 1.5 percent water due to 82°C and 95 percent relative humidity and suffer a 10 to 15 percent decrease in flexural strength. Thus, the effects of moisture absorption on the flexural strength of

carbon/bismaleimide are of the same general nature to like effects on carbon/epoxy, although somewhat less moisture has a more deleterious effect on the strength of carbon/bismaleimide.

SUMMARY

Characterization of the fracture behavior and flexural properties of carbon fiber cross-ply laminates has shown the following:

1. Center-notched panels of carbon/epoxy and 90₂/0 orientations of carbon/bismaleimide showed linear elastic translaminar fracture at K_{max} values up to about 30 MPa m^{1/2}. Carbon/bismaleimide panels with a larger share of 0-degree fibers showed mixed translaminar and interlaminar splitting fracture and considerable permanent deformation, at K_{max} values of 45 to 90 MPa m^{1/2} and K_{Jmax} values up to 400 MPa m^{1/2}.
2. Significant environmental effects on fracture were noted for 0₂/90 carbon/bismaleimide following 85°C and 97 percent relative humidity chamber exposure, causing a 20 percent decrease in K_{max} from 92 to 74 MPa m^{1/2}.
3. Scanning electron microscope fractography showed clear distinctions between the low toughness carbon/epoxy, which had a relatively featureless fracture surface with no fiber pullout, and the high toughness carbon/bismaleimide, which had a rough surface and extensive fiber pullout.
4. Flexural strength and modulus for both types of laminate varied between 300 and 700 MPa and 30 and 100 GPa, respectively, with higher values for higher shares of 0-degree fibers. A significant decrease in flexural strength was noted for 0₂/90 carbon/bismaleimide following moisture chamber exposure, causing an 18 percent decrease from 486 to 397 MPa.

Evaluation and development of test procedures to determine fracture and flexural properties of the laminates have shown the following:

1. The center-notch tensile panel was entirely suitable for fracture toughness tests of carbon fiber laminates. Expressions for K, J, and displacement were identified and modified. Notch configuration effects on test results were small.

2. Interlaminar splitting at the notch tips was critical, being both the cause and a convenient indicator of the high toughness mode of deformation and fracture for these carbon fiber laminates.

3. The source of a significant error in flexure testing was identified as rotation of the loading pins relative to the specimen. An expression was given which can be used to include effects of rotation in calculating strength and modulus.

REFERENCES

1. J.H. Underwood, written discussion of "Damage Mechanics Analysis of Matrix Effects in Notched Laminates," by C.-G. Aronsson and J. Backlund, Composite Materials: Fatigue and Fracture, ASTM STP 907, (H.T. Hahn, ed.), American Society for Testing and Materials, Philadelphia, 1986, pp. 156-157.
2. T.K. O'Brien, N.J. Johnson, R.S. Raju, D.M. Morris, and R.A. Simonds, "Comparisons of Various Configurations of the Edge Delamination Test for Interlaminar Fracture Toughness," Toughened Composites, ASTM STP 937, (Norman J. Johnson, ed.), American Society for Testing and Materials, Philadelphia, 1988, pp. 199-221.
3. C.E. Anderson, J.W. Cardinal, and M.F. Kanninen, "A Fracture Mechanics Analysis for the Failure of Filament-Wound Pressurized Containers Subjected to Intense Energy Deposition," Lightening The Force - The Role of Mechanics, Proceedings of Army Symposium on Solid Mechanics, West Point, NY, 1986.
4. S. Bandyopadhyay, E.P. Gellert, V.M. Silva, and J.H. Underwood, "Microscopic Aspects of Failure and Fracture in Cross-Ply Fibre-Reinforced Composite Laminates," J. of Composite Materials, Vol. 23, December 1989, pp. 1216-1231; also, ARCCB-TR-88040, Benet Laboratories, Watervliet, NY, November 1988.
5. C.E. Feddersen, "Evaluation and Prediction of the Residual Strength of Center Cracked Tension Panels," Damage Tolerance in Aircraft Structures, ASTM STP 486, American Society for Testing and Materials, Philadelphia, PA, 1971, pp. 50-78.
6. H. Tada, P.C. Paris, and G.R. Irwin, The Stress Analysis of Cracks Handbook, Paris Productions, Inc., St. Louis, MO, 1985, pp. 11.1-11.2.

7. H. Tada, P.C. Paris, and G.R. Irwin, The Stress Analysis of Cracks Handbook, Paris Productions, Inc., St. Louis, MO, 1985, pp. 2.4-2.5.
8. J.C. Newman, Jr., "Crack-Opening Displacements in Center-Crack, Compact, and Crack-Line Wedge-Loaded Specimens," NASA TN D-8268, NASA Langley Research Center, Hampton, VA, July 1976.
9. R.J. Roark and W.C. Young, Formulas for Stress and Strain, McGraw-Hill, New York, 1975, pp. 96-108.
10. J.R. Rice, P.C. Paris, and J.G. Merkle, "Some Further Results of J-Integral Analysis and Estimates," Progress in Flaw Growth and Fracture Toughness Testing, ASTM STP 536, American Society for Testing and Materials, 1973, pp. 231-245.
11. T.H. Mao, "Tensile Fracture of Graphite/Epoxy Laminates with Central Crack," Proceedings of the Fifth International Conference on Composite Materials, (W.C. Harrigan, Jr., J. Strife, and A.K. Dhingra, eds.), The Metallurgical Society, 1985, pp. 383-390.
12. S. Bandyopadhyay and P.N. Murthy, "Experimental Studies on Interfacial Shear Strength in Glass Fibre Reinforced Plastics Systems," Materials Science and Engineering, Vol. 19, No. 1, May 1975, pp. 139-145.
13. A.G. Evans and D.B. Marshall, "Mechanical Behavior of Ceramic Matrix Composites," plenary lecture, Seventh International Conference on Fracture, Houston, TX, 1989.
14. G.S. Springer, "Moisture and Temperature Induced Degradation of Graphite Epoxy Composites," in: Environmental Effects on Composite Materials, (George S. Springer, ed.), Technomic Publishing Co., Lancaster, PA, 1984, pp. 6-19.

TABLE I. MATERIAL AND TEST CONDITIONS

Matrix	Layers	Thickness 8 mm	Orientation	Environment Prior To Test		
				Lab Air	Moisture Chamber	Tropical Exposure
epoxy	7	1.1	0/90	X	-	-
epoxy	7	1.1	0/ \pm 60	X	-	-
epoxy	7	1.1	90/0	X	-	-
bismaleimide	11	1.8	0/90	X	X	X
bismaleimide	11	1.8	90/0	X	-	-
bismaleimide	11	1.8	0 ₂ /90	X	X	X
bismaleimide	11	1.8	90 ₂ /0	X	X	-

TABLE II. SUMMARY OF FRACTURE TOUGHNESS TESTS

Material	Notch Length 2a/W	Notch Radius r mm	Environment	Behavior	Fracture Toughness* K_{max} MPa $\text{m}^{1/2}$	K_{Jmax}
0/±60 Ep**	0.51	0.02-0.3	laboratory	linear	22.6(1.4)	-
	0.50	3.0	laboratory	linear	29.1(2.0)	-
0/90 Ep	0.3-0.7	0.15-0.3	laboratory	linear	19.2(3.3)	-
	0.37	bullet	laboratory	linear	21.4(1.7)	-
90/0 Ep	0.49	0.3	laboratory	linear	16.6(1.6)	-
0/90 Bs**	0.67	0.3	laboratory	splits	84.1(0.4)	349(30)
	0.68	0.3	chamber	splits	85.8(2.8)	364(32)
	0.68	0.3	tropical	splits	84.1(8.2)	281(99)
90/0 Bs	0.68	0.3	laboratory	nonlinear	45.3(2.3)	--
0 ₂ /90 Bs	0.50	0.3	laboratory	splits	57.7(15.8)	283(80)
	0.67	0.3	laboratory	splits	92.2(6.4)	425(55)
	0.69	0.3	chamber	splits	74.4(6.7)	344(46)
	0.65	0.3	tropical	splits	89.5(1.2)	328(78)
90 ₂ /0 Bs	0.68	0.3	laboratory	linear	26.4(1.3)	--
	0.67	0.3	chamber	linear	29.7(2.0)	--

*Mean value of three replicates; standard deviation indicated ()

**Ep - Epoxy, Bs - Bismaleimide

TABLE III. SUMMARY OF FLEXURAL STRENGTH AND FLEXURAL MODULUS TESTS

Material	Environment	Flexural Strength* S_B MPa	Flexural Modulus* E_B GPa
0/±60 Ep**	laboratory	678(22)	82.4(3.8)
0/90 Ep	laboratory	691(11)	85.0(1.8)
90/0 Ep	laboratory	414(12)	53.1(1.0)
0/90 Bs**	laboratory	482(43)	89.0(8.7)
	chamber	491(96)	87.0(14.0)
	tropical	484(30)	82.5(11.0)
90/0 Bs	laboratory	473(33)	63.0(1.7)
0 ₂ /90 Bs	laboratory	486(39)	101.3(17.0)
	chamber	397(78)	88.0(24.1)
	tropical	473(71)	90.3(9.0)
90 ₂ /0 Bs	laboratory	279(23)	32.7(4.0)
	chamber	300(14)	33.3(3.2)

*Mean value of three replicates; standard deviation indicated ()

**Ep - Epoxy, Bs - Bismaleimide

TABLE IV. PLY ORIENTATION EFFECT ON FRACTURE TOUGHNESS

Material	Notch Length 2a/W	Fracture Toughness K_{max} , MPa $\text{m}^{1/2}$	Ratio of K_{max}	Ratio of 0° Plies
0/90 Ep*	0.50	20.0	-	-
90/0 Ep	0.49	16.6	0.83	0.75
0/90 Bs*	0.67	84.1	-	-
90/0 Bs	0.68	45.3	0.54	0.83
0 ₂ /90 Bs	0.67	92.2	-	-
90 ₂ /0 Bs	0.68	26.4	0.29	0.27

*Ep - Epoxy, Bs - Bismaleimide

TABLE V. ENVIRONMENTAL EFFECTS ON FRACTURE TOUGHNESS FOR
CARBON/BISMALEIMIDE; NOMINAL $2a/W = 0.67$, $r = 0.3$ mm

Orientation	Environment	Fracture Toughness K_{max} MPa $m^{1/2}$	Difference in Fracture Toughness MPa $m^{1/2}$	Largest Standard Deviation MPa $m^{1/2}$
0/90	laboratory	84.1	-	-
	chamber	85.8	1.7	2.8
	tropical	84.1	0.0	8.2
0 ₂ /90	laboratory	92.2	-	-
	chamber	74.4	17.8	6.7
	tropical	89.5	2.7	6.4
90 ₂ /0	laboratory	26.4	-	-
	chamber	29.7	3.3	2.0

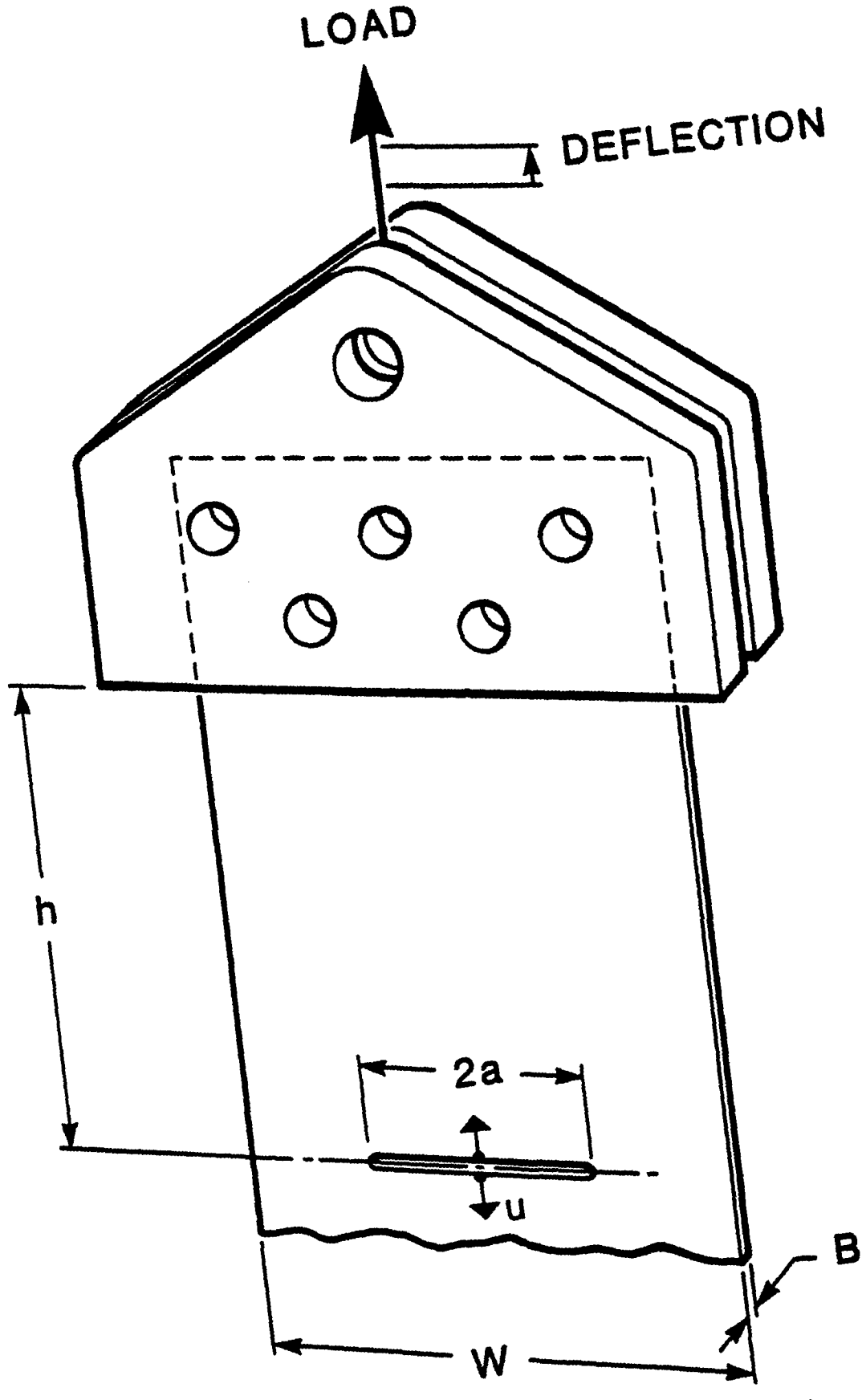


Figure 1. Fracture toughness test arrangement.

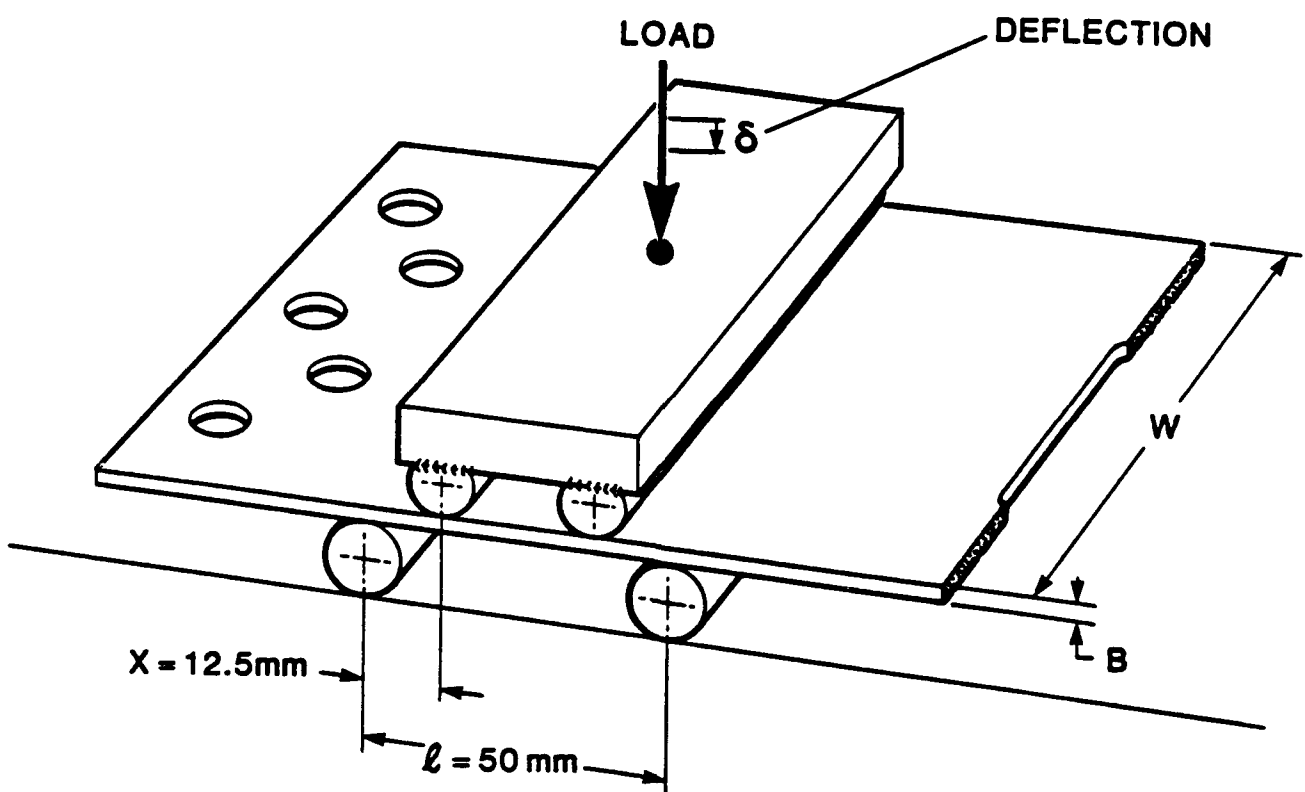


Figure 2. Flexural strength and modulus test arrangement.

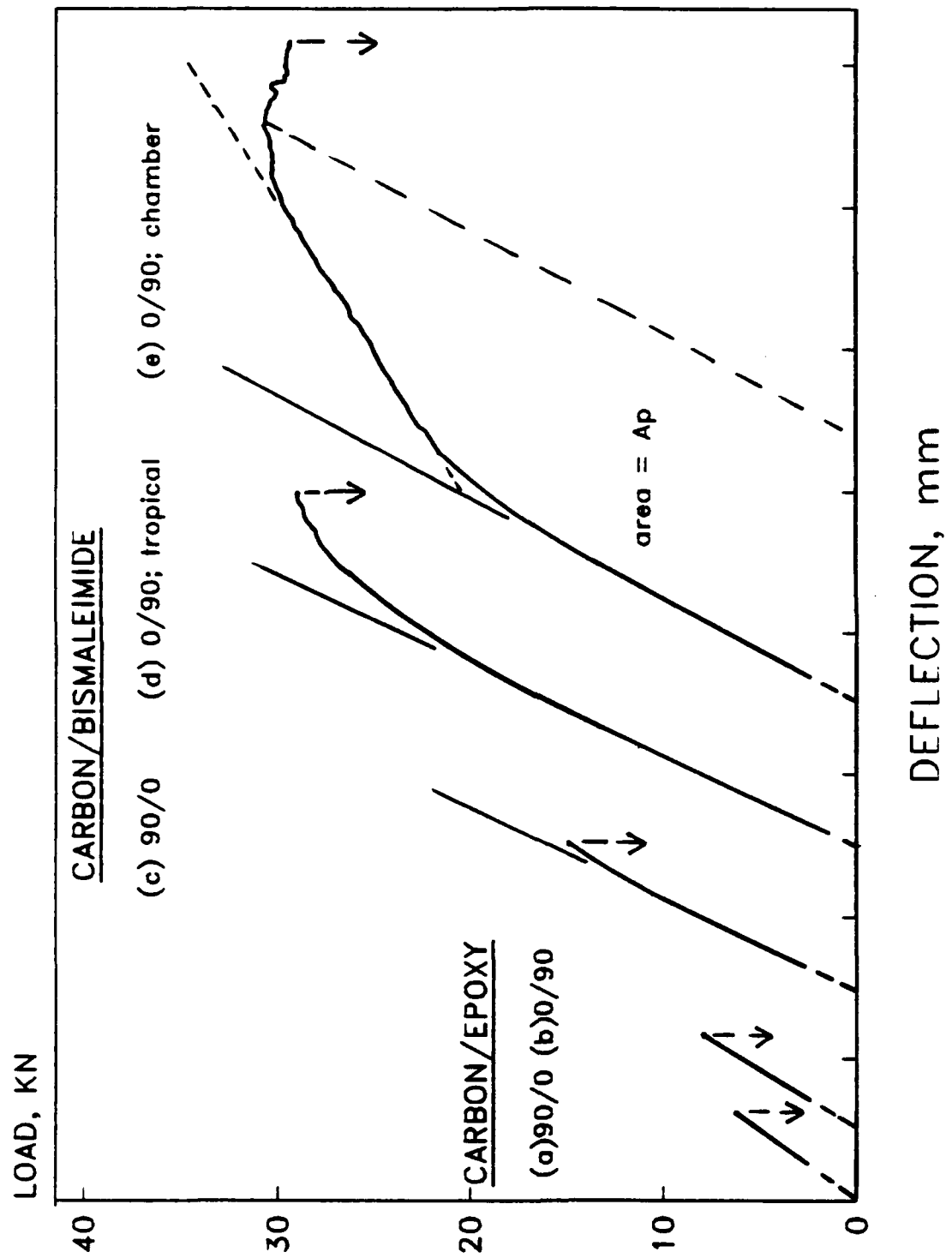


Figure 3. Load versus deflection behavior of notched tensile panels.

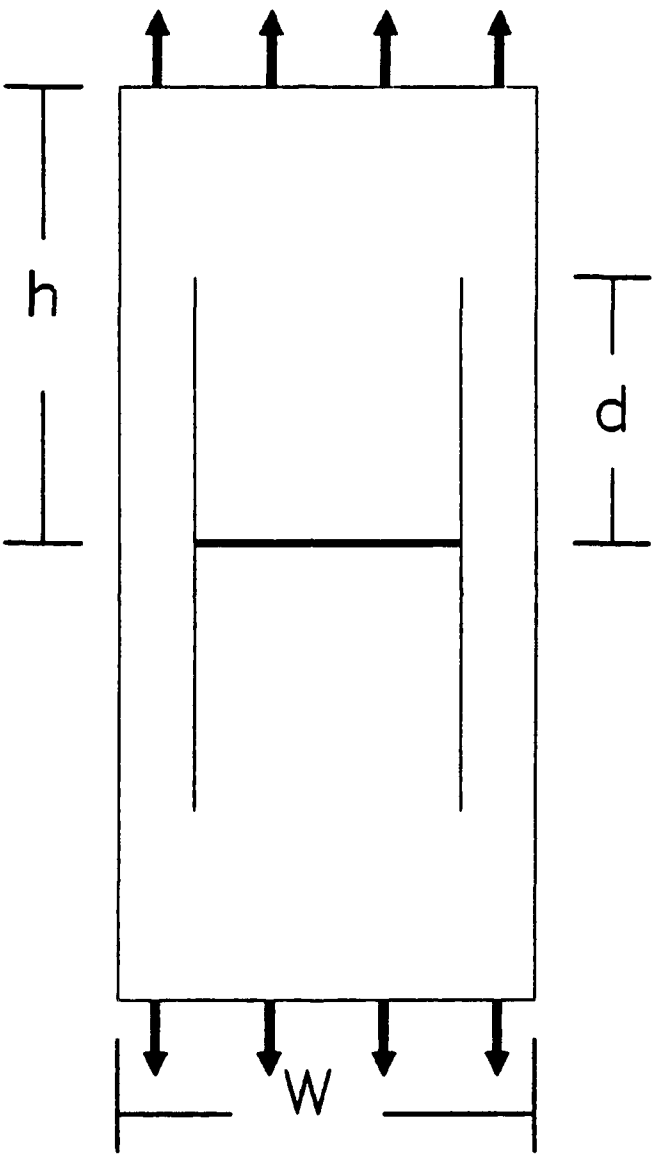


Figure 4. Typical splitting of 0/90 and 0₂/90 carbon/bismaleimide panels.

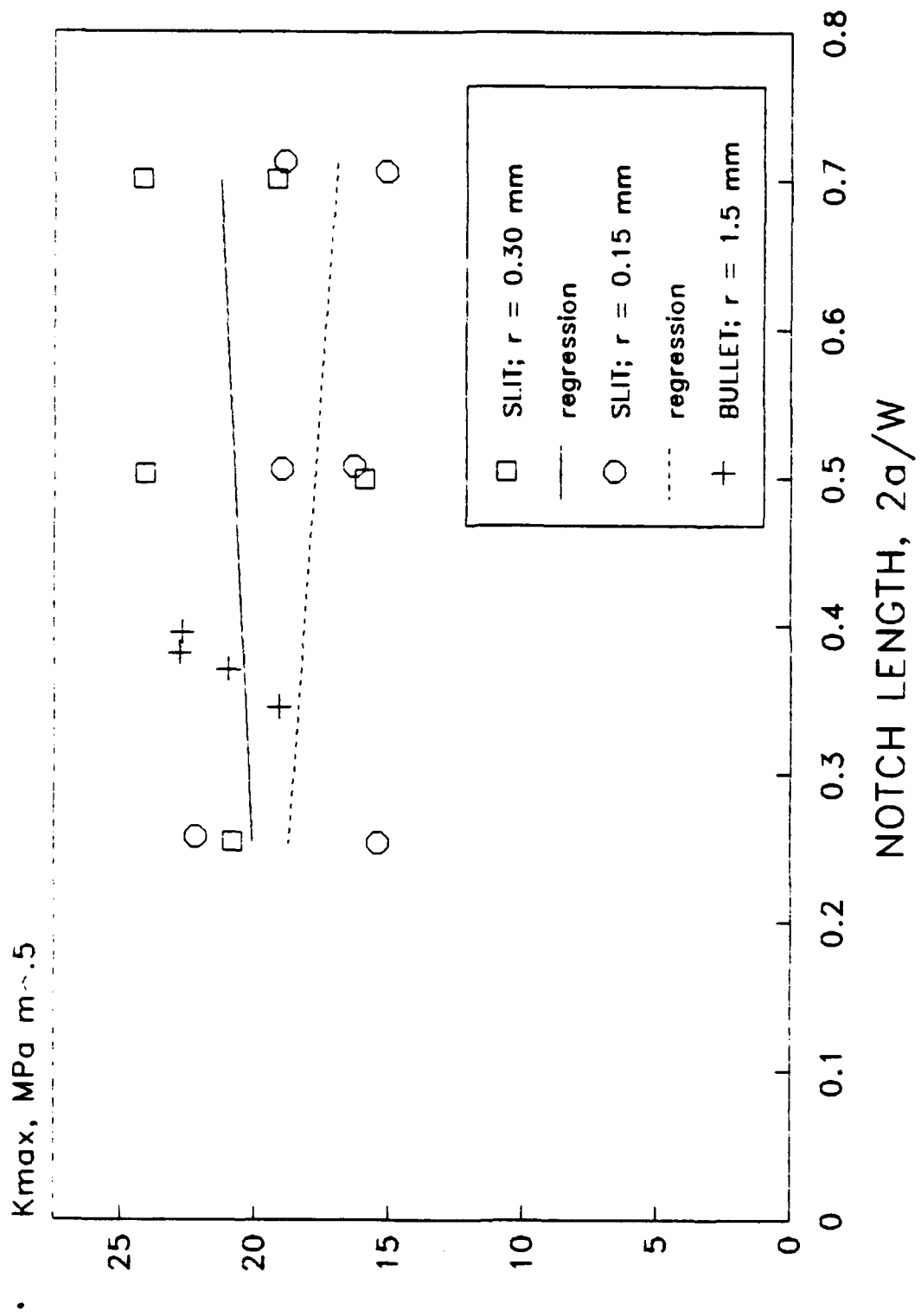


Figure 5. Effects of notch configuration on fracture toughness for 0/90 carbon/epoxy.

10

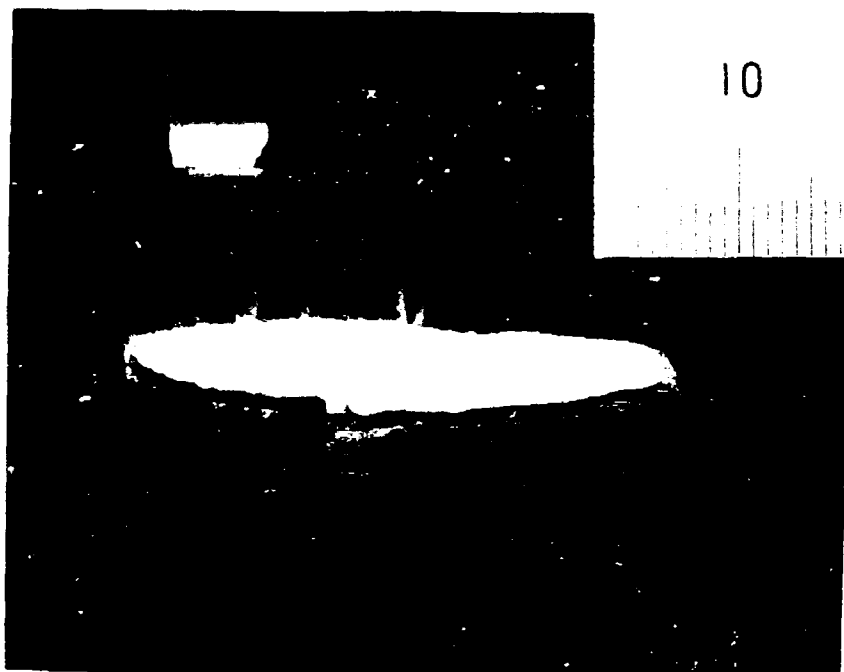


Figure 6. Photograph of 0/90 carbon/epoxy panel with ballistic penetration, pieced together after tensile loading to failure; penetrator also shown.

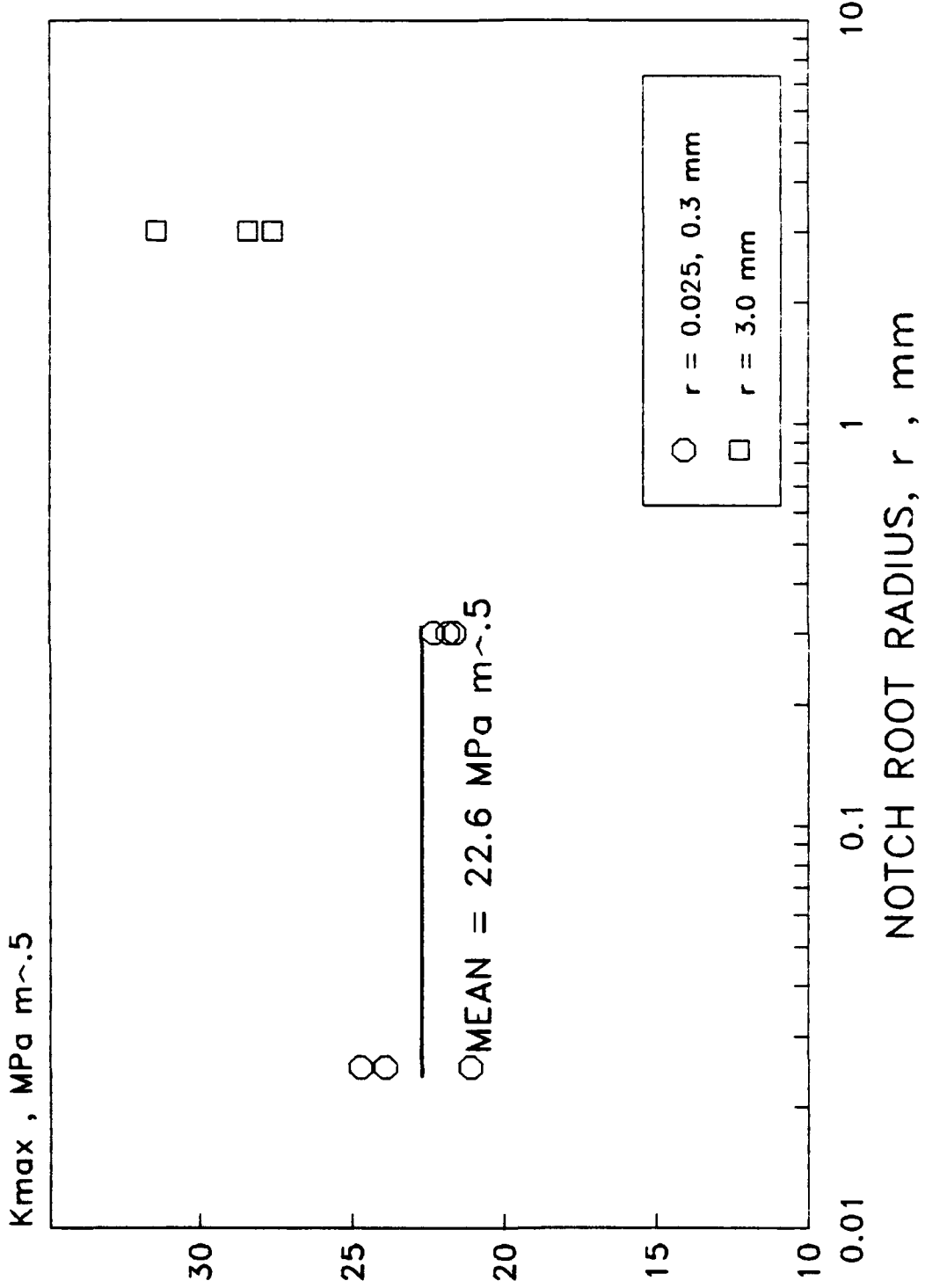
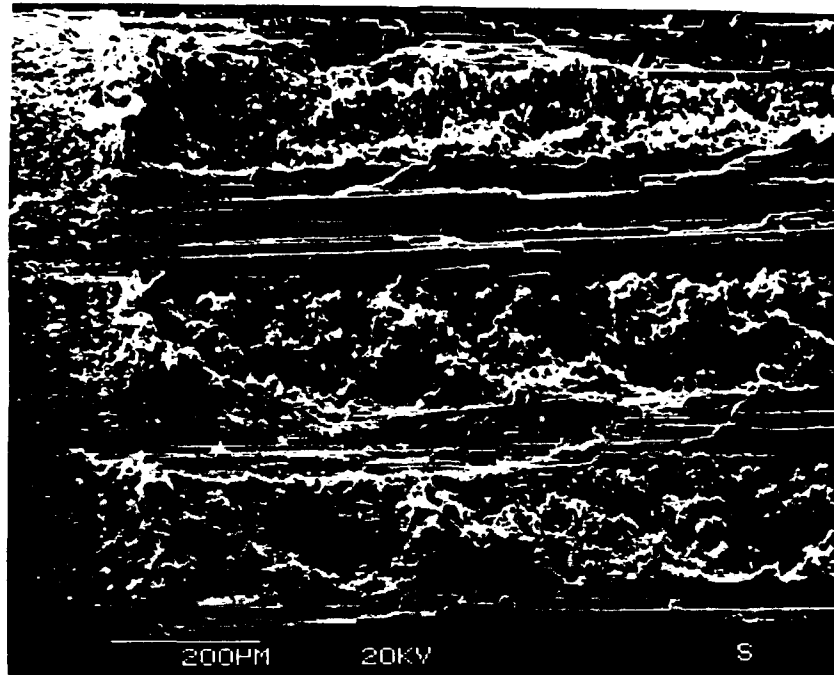
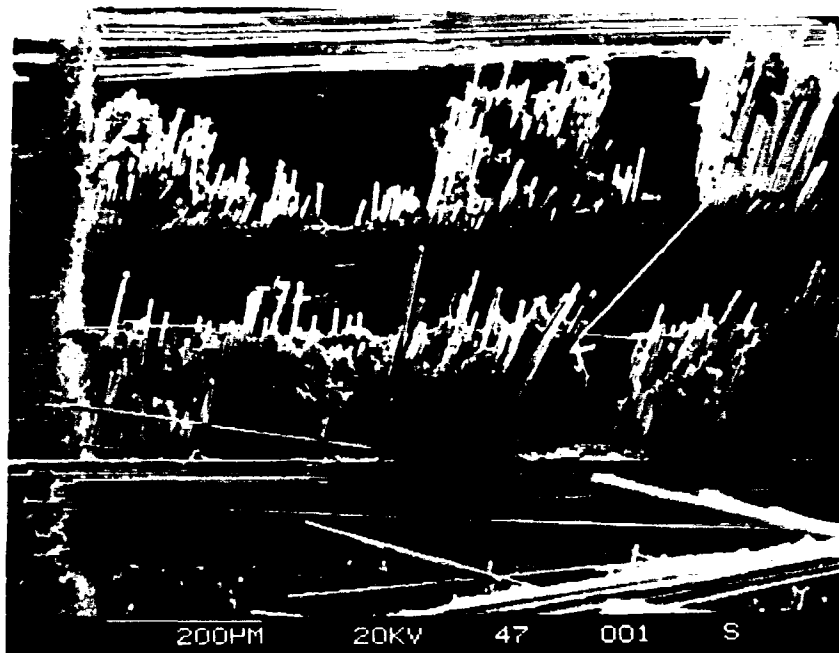


Figure 7. Effects of notch radius on fracture toughness for 0/t60 carbon/epoxy; nominal $2a/W = 0.5$.

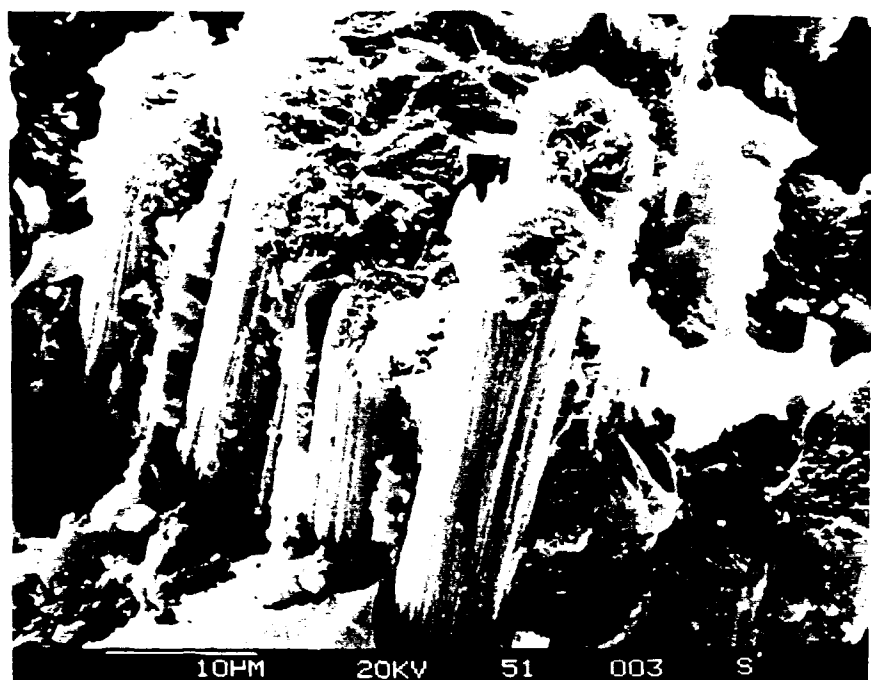


(a) 90/0 carbon/epoxy, little fiber pullout.



(b) 90/0 carbon/bismaleimide, extensive fiber pullout.

Figure 8. Low magnification SEM fractographs at notch tip.



(a) 90/0 carbon/epoxy, predominantly failure of fiber bundles.



(b) 90/0 carbon/bismaleimide, predominantly pullout of individual fibers.

Figure 9. High magnification SEM fractographs 3 mm from notch tip.

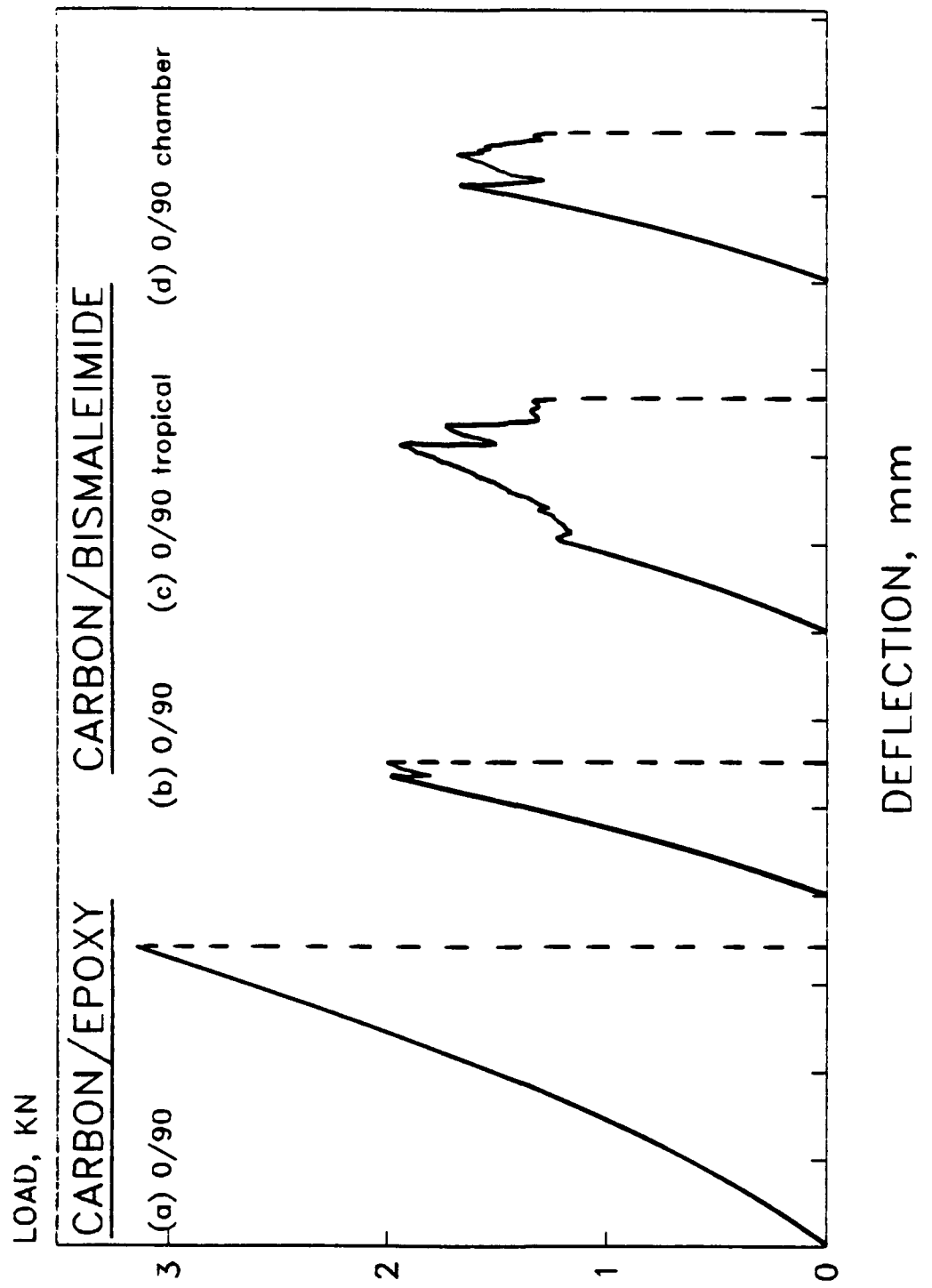


Figure 10. Load versus deflection behavior of flexure specimens.

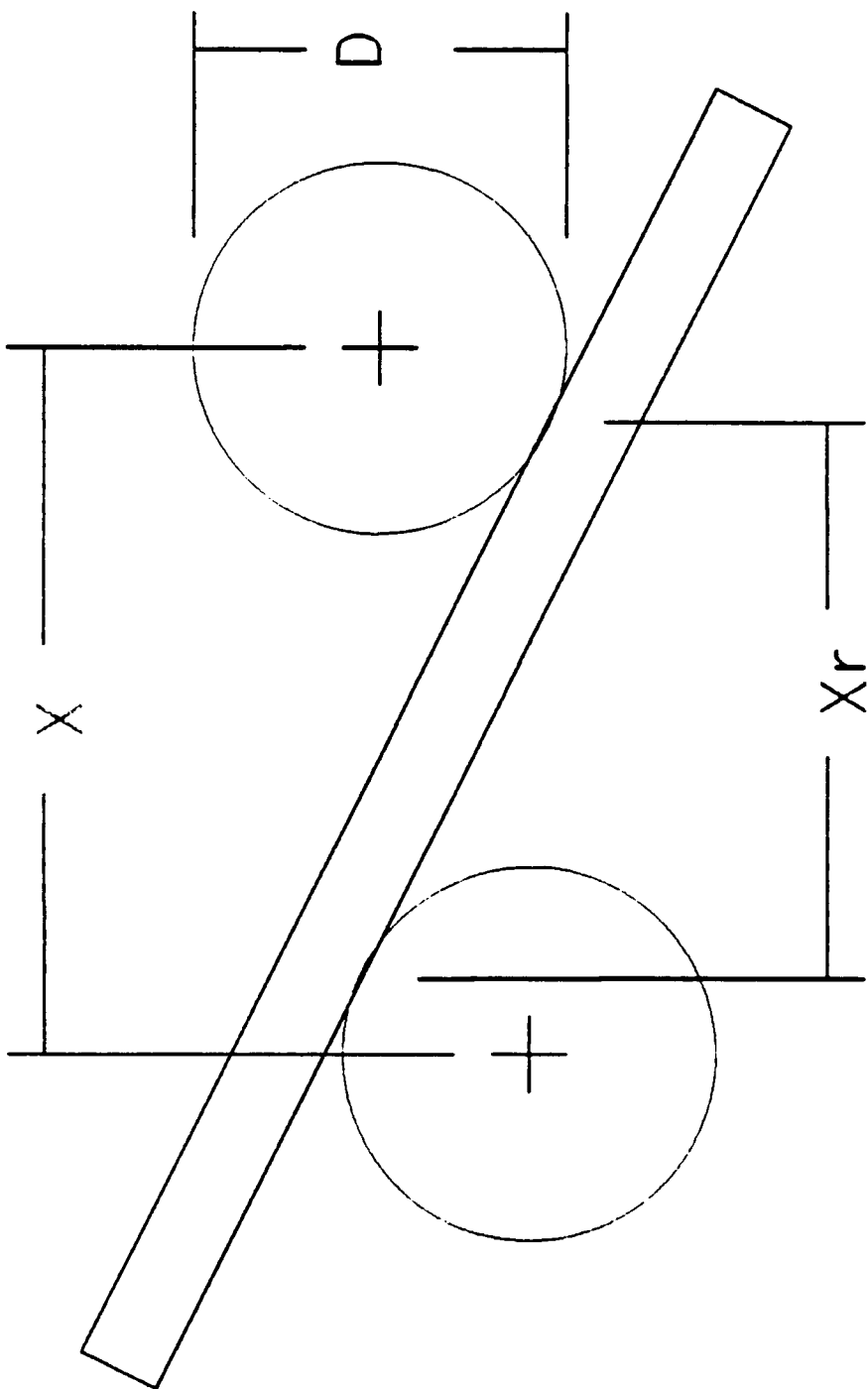


Figure 11. Rotation of loading pins relative to flexure specimens.

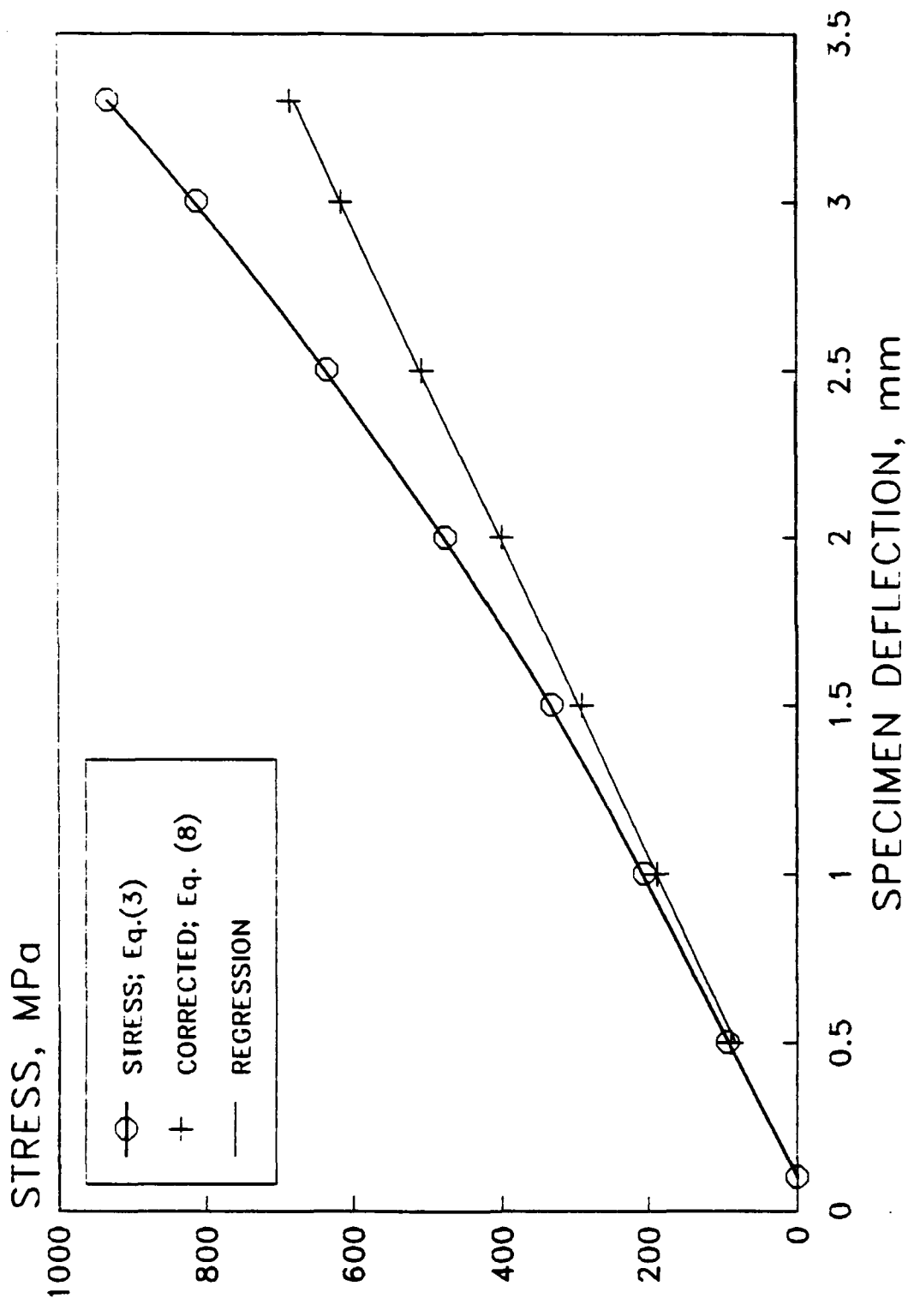


Figure 12. Flexural stress versus specimen deflection showing correction for rotation.

TECHNICAL REPORT INTERNAL DISTRIBUTION LIST

	<u>NO. OF COPIES</u>
CHIEF, DEVELOPMENT ENGINEERING DIVISION ATTN: SMCAR-CCB-D	1
-DA	1
-DC	1
-DI	1
-DP	1
-DR	1
-DS (SYSTEMS)	1
CHIEF, ENGINEERING SUPPORT DIVISION ATTN: SMCAR-CCB-S	1
-SE	1
CHIEF, RESEARCH DIVISION ATTN: SMCAR-CCB-R	2
-RA	1
-RE	1
-RM	1
-RP	1
-RT	1
TECHNICAL LIBRARY ATTN: SMCAR-CCB-TL	5
TECHNICAL PUBLICATIONS & EDITING SECTION ATTN: SMCAR-CCB-TL	3
DIRECTOR, OPERATIONS DIRECTORATE ATTN: SMCWV-OD	1
DIRECTOR, PROCUREMENT DIRECTORATE ATTN: SMCWV-PP	1
DIRECTOR, PRODUCT ASSURANCE DIRECTORATE ATTN: SMCWV-QA	1

NOTE: PLEASE NOTIFY DIRECTOR, BENET LABORATORIES, ATTN: SMCAR-CCB-TL, OF ANY ADDRESS CHANGES.

TECHNICAL REPORT EXTERNAL DISTRIBUTION LIST

	<u>NO. OF COPIES</u>		<u>NO. OF COPIES</u>
ASST SEC OF THE ARMY RESEARCH AND DEVELOPMENT ATTN: DEPT FOR SCI AND TECH THE PENTAGON WASHINGTON, D.C. 20310-0103	1	COMMANDER ROCK ISLAND ARSENAL ATTN: SMCRI-ENM ROCK ISLAND, IL 61299-5000	1
ADMINISTRATOR DEFENSE TECHNICAL INFO CENTER ATTN: DTIC-FDAC CAMERON STATION ALEXANDRIA, VA 22304-6145	12	DIRECTOR US ARMY INDUSTRIAL BASE ENGR ACTV ATTN: AMXIB-P ROCK ISLAND, IL 61299-7260	1
COMMANDER US ARMY ARDEC ATTN: SMCAR-AEE SMCAR-AES, BLDG. 321 SMCAR-AET-0, BLDG. 351N SMCAR-CC SMCAR-CCP-A SMCAR-FSA SMCAR-FSM-E SMCAR-FSS-D, BLDG. 94 SMCAR-IMI-I (STINFO) BLDG. 59 PICATINNY ARSENAL, NJ 07806-5000	1 1 1 1 1 1 1 1 2	COMMANDER US ARMY TANK-AUTMV R&D COMMAND ATTN: AMSTA-DDL (TECH LIB) WARREN, MI 48397-5000	1
DIRECTOR US ARMY BALLISTIC RESEARCH LABORATORY ATTN: SLCBR-DD-T, BLDG. 305 ABERDEEN PROVING GROUND, MD 21005-5066	1	COMMANDER US MILITARY ACADEMY ATTN: DEPARTMENT OF MECHANICS WEST POINT, NY 10996-1792	1
DIRECTOR US ARMY MATERIEL SYSTEMS ANALYSIS ACTV ATTN: AMXSY-MP ABERDEEN PROVING GROUND, MD 21005-5071	1	US ARMY MISSILE COMMAND REDSTONE SCIENTIFIC INFO CTR ATTN: DOCUMENTS SECT, BLDG. 4484 REDSTONE ARSENAL, AL 35898-5241	2
COMMANDER HQ, AMCCOM ATTN: AMSMC-IMP-L ROCK ISLAND, IL 61299-6000	1	COMMANDER US ARMY FGN SCIENCE AND TECH CTR ATTN: DRXST-SD 220 7TH STREET, N.E. CHARLOTTESVILLE, VA 22901	1
		COMMANDER US ARMY LABCOM MATERIALS TECHNOLOGY LAB ATTN: SLCMT-IML (TECH LIB) WATERTOWN, MA 02172-0001	2

NOTE: PLEASE NOTIFY COMMANDER, ARMAMENT RESEARCH, DEVELOPMENT, AND ENGINEERING CENTER, US ARMY AMCCOM, ATTN: BENET LABORATORIES, SMCAR-CCB-TL, WATERVLIET, NY 12189-4050, OF ANY ADDRESS CHANGES.

TECHNICAL REPORT EXTERNAL DISTRIBUTION LIST (CONT'D)

<u>NO. OF COPIES</u>	<u>NO. OF COPIES</u>		
COMMANDER US ARMY LABCOM, ISA ATTN: SLCIS-IM-TL 2800 POWDER MILL ROAD ADELPHI, MD 20783-1145	1	COMMANDER AIR FORCE ARMAMENT LABORATORY ATTN: AFATL/MN EGLIN AFB, FL 32542-5434	1
COMMANDER US ARMY RESEARCH OFFICE ATTN: CHIEF, IPO P.O. BOX 12211 RESEARCH TRIANGLE PARK, NC 27709-2211	1	COMMANDER AIR FORCE ARMAMENT LABORATORY ATTN: AFATL/MNF EGLIN AFB, FL 32542-5434	1
DIRECTOR US NAVAL RESEARCH LAB ATTN: MATERIALS SCI & TECH DIVISION CODE 26-27 (DOC LIB) WASHINGTON, D.C. 20375	1	METALS AND CERAMICS INFO CTR BATTELLE COLUMBUS DIVISION 505 KING AVENUE COLUMBUS, OH 43201-2693	1
DIRECTOR US ARMY BALLISTIC RESEARCH LABORATORY ATTN: SLCBR-IB-M (DR. BRUCE BURNS) ABERDEEN PROVING GROUND, MD 21005-5066	1		

NOTE: PLEASE NOTIFY COMMANDER, ARMAMENT RESEARCH, DEVELOPMENT, AND ENGINEERING CENTER, US ARMY AMCCOM, ATTN: BENET LABORATORIES, SMCAR-CCB-TL, WATERVLIET, NY 12189-4050, OF ANY ADDRESS CHANGES.